

Research Article

Performance of Narrowband Signal Detection under Correlated Rayleigh Fading Based on Synthetic Array

Ali Broumandan, John Nielsen, and Gérard Lachapelle

Position Location and Navigation (PLAN) Group, Schulich School of Engineering, University of Calgary,
2500 University Drive, N.W., Calgary, AB, Canada T2N 1N4

Correspondence should be addressed to Ali Broumandan, abrouman@ucalgary.ca

Received 1 April 2009; Revised 15 July 2009; Accepted 27 July 2009

Recommended by Hon Tat Hui

The performance of a single moving antenna receiver in detecting a narrowband signal under correlated Rayleigh fading is considered. The spatial motion of the antenna during signal capture provides a realization of a synthetic antenna array. As shown, there is a net processing gain obtained by using a synthetic antenna array compared to the equivalent static antenna in Rayleigh fading environments subject to constant processing time. The performance analysis is based on average Signal-to-Noise Ratio (SNR) metrics for design parameters of probability of detection (P_d) and probability of false alarm (P_{fa}). An optimum detector based on Estimator-Correlator (EC) is developed, and its performance is compared with that of suboptimal Equal-Gain (EG) combiner in different channel correlation scenarios. It is shown that in moderate channel correlation scenarios the detection performance of EC and EG is identical. The sensitivity of the proposed method to knowledge of motion parameters is also investigated. An extensive set of measurements based on CDMA-2000 pilot signals using the static antenna and synthetic array are used to experimentally verify these theoretical findings.

Copyright © 2009 Ali Broumandan et al. This is an open access article distributed under the Creative Commons Attribution License, which permits unrestricted use, distribution, and reproduction in any medium, provided the original work is properly cited.

1. Introduction

In a wireless mobile communication system, signals propagate from the transmitter to the receiver over multiple paths resulting in multipath fading. When there is no line of sight (LOS) path available from the transmitter and an antenna is located in a dense scattering environment (e.g., indoor and urban environments), the multipath fading appears to be spatially random conforming to Rayleigh statistics [1, 2]. A characteristic of multipath fading is fluctuations in received signal strength as a function of spatial dimensions, which results in signal reception problems for a static antenna. The use of multiple antennas can alleviate the fading problem to some degree by providing a means of diversity gain [3–5]. Diversity techniques are established based on receiving statistically independent signals on each diversity antenna denoted as diversity branch. In practice, this may be implemented by utilizing spatially separated antennas in dense multipath environments, which results in spatial diversity [6–8] or by utilizing antennas with different polarizations that map

into polarization diversity [9]. A performance comparison of the spatial diversity and the polarization diversity in Rayleigh fading environment is investigated in [10]. The performance of a diversity system can be characterized by the correlation coefficient value among diversity branches. In the multipath fading environment, the correlation coefficient decreases spatially where the decorrelation rate depends on the geometry of the scatterers and array configuration. If multipath components arrive from a small sector in space, the antenna elements should have spacing on order of several wavelengths of the carrier frequency to yield spatial diversity, whereas in the ring of scatterers multipath model, less than half wavelength spacing is sufficient to ensure spatially uncorrelated samples. Hence, spatial correlation matrix is a function of channel model and antenna spacing. The performance of diversity systems reduces by increasing the correlation coefficient among diversity branches.

As stated before, an antenna array with multiple elements that samples the spatial field with statistically independent

samples can be considered as a diversity system. Unfortunately, the physical size of antenna array necessary for achieving a reasonable spatial diversity gain is several carrier wavelengths, which is incompatible with the small form factors of typical handheld receiver devices. To overcome this size restriction, a single antenna can be physically moved while the receiver is capturing the signal, thereby realizing a synthetic antenna array. The mobile station (MS) operator may move the handheld receiver in an arbitrary trajectory or else the MS can be attached to a moving platform such as a vehicle. The concept of a synthetic array based on a single moving antenna has been utilized in wireless signal parameter estimation and radar signal processing [11, 12]. In previous work, antenna trajectories have either been mechanically fixed or precisely measured during the signal snapshot using accurate inertial navigation devices [12, 13] which restricts portability and applicability of implementation in handset receivers.

Authors in [14] have proposed a new method for detecting a narrowband signal in uncorrelated Rayleigh fading based on the synthetic array concept. In [14] the detection performance of a single channel receiver based on a moving antenna is compared to that of the equivalent receiver with a stationary antenna based on the diversity gain as a quantifiable metric. It is shown that if the antenna is held at a fixed position during the snapshot interval, then the signal is not subject to decorrelation. However, the signal will be subject to fading losses, which are statistically large in a Rayleigh fading environment. Conversely, if the antenna is translated along some arbitrary trajectory during the snapshot interval, then the coherency of the signal will be compromised as the channel gain will change randomly but the snapshot data will contain spatial diversity that can effectively counter the spatial fading effects. Based on this, it is shown that the tradeoff between increased diversity gain and loss of signal coherency will result in an optimum processing gain.

The primary assumption of previous work related to the spatial diversity gain was based on uncorrelated spatial signal samples that resulted in the Equal-Gain (EG) combining [14–16]. While this is optimum for uncorrelated Rayleigh fading, it is not optimum when the fading is spatially correlated [17]. However, in the synthetic array context uncorrelated spatial sample assumption is valid when the trajectory of the moving antenna and channel statistics are known. Authors in [18] have taken into account the performance degradation of the synthetic array in the correlated Rayleigh fading.

In this paper, the achievable processing gain of a synthetic array antenna where the single antenna is translated through an arbitrary trajectory of spatially correlated Rayleigh faded signal is analyzed. The net processing gain of the synthetic array antenna based on optimum estimator-correlator (EC) combining is contrasted with that of the static antenna in an equivalently faded propagation environment. The processing gain advantage of the EC is also compared with the EG combining for a range of spatial correlation. The sensitivity of the proposed method in terms of the trajectory estimation is also considered. The environment of interest is indoor

where there is no well-defined LOS component and the multipath is diffuse. In addition, the signal bandwidth is narrow such that it is assumed to be less than the coherence bandwidth resulting in unresolved multipath components. The quantitative metric that is used for comparison is the SNR required at the receiver to achieve specific detection performance goals. That is target values of the probability of detection (P_d) and probability of false alarm (P_{fa}) are fixed. The required SNR to achieve this detection performance is compared for the synthetic array with EG and EC combining and the static antenna. The required SNR is initially determined theoretically based on the assumption of Rayleigh fading. Subsequently, experimental measurements based on CDMA-2000 pilot signals propagated from an outdoor BS and received indoor are utilized to partially validate the theoretical conclusions.

The paper is organized as follows. In Section 2, the static antenna system model is given along with theoretical performances. In Section 3, the synthetic array system model with EC and EG combining is described. In Section 4, the processing gain advantage of the synthetic array based on the EC and EG combining in correlated Rayleigh fading is contrasted with the static antenna. The practical implementation issues of the synthetic array are also given in Section 4. Experimental measurement results are given in Section 5. Section 6 concludes the paper.

2. Static Antenna System Model and Detection Performance

Consider $r(t)$ as a complex baseband signal received by a single antenna, which is processed to decode between two states, H_0 , where only noise is present, and H_1 where both signal and noise are present. The representation of $r(t)$ for a static antenna located at position \mathbf{p} is

$$r(t) = A(\mathbf{p})s_0(t) + w(t), \quad (1)$$

where $s_0(t)$ is the deterministic complex baseband component of the signal that is known to the receiver, and $A(\mathbf{p})$ is the channel gain as a function of spatial position. The channel gain is assumed to be temporally static during the time interval where the data is collected. However, the channel gain varies randomly with the spatial variable \mathbf{p} according to the assumed Rayleigh fading. Hence, $A(\mathbf{p})$ is assumed to be a zero mean circular normal random variable such that $A(\mathbf{p}) \sim \text{CN}(0, \sigma_A^2)$ where \sim denotes the Probability Density Function (PDF) of the left-hand side variable, and $\text{CN}(0, \sigma^2)$ signifies a zero mean circular normal PDF with variance σ^2 . (Random variable $B = u + jv$ distributed according to circularly normal PDF with zero mean and variance σ^2 , $\text{CN}(0, \sigma^2)$, where u and v are independent zero-mean normal random variables each with variance $\sigma^2/2$, $u \sim N(0, \sigma^2/2)$ and $v \sim N(0, \sigma^2/2)$.) The received signal is corrupted with additive noise denoted by $w(t)$, which is assumed to be circularly normal and spectrally white within the signal bandwidth of $s_0(t)$ with a double sided power spectral density of $N_0/2$. The static antenna receiver accumulates a temporal snapshot of $r(t)$ over the snapshot

interval of $t \in [0, T]$. Based on these assumptions, the optimal Neyman-Pearson (NP) detection processing is a matched filter based on correlation with $s_0(t)^*$ followed by a magnitude squared operation [17]. This processing results in the decision variable as z_s which is expressed as [19]

$$z_s = \left| \frac{1}{T} \int_0^T r(t) s_0(t)^* dt \right|^2 = |x_s|^2, \quad (2)$$

where $x_s = (1/T) \int_0^T r(t) s_0(t)^* dt$ and subscript s signifies static processing case. For convenience the signal energy of $s_0(t)$ is normalized as $(1/T) \int_0^T |s_0(t)|^2 dt = 1$. The noise at the output of the processor is circularly normal as $\int_0^T w(t) s_0(t)^* dt \sim \text{CN}(0, TN_o)$. Based on this it is convenient to define ρ as the average signal-to-noise ratio as

$$\rho \equiv \frac{\sigma_A^2}{\sigma_w^2} = \frac{T\sigma_A^2}{N_o}, \quad (3)$$

where $\sigma_w^2 = N_o/T$ is the noise variance at the output of the correlation process. This definition will be used throughout the remainder of the paper. Without loss of generality, the normalization of $TN_o = 1$ can be imposed such that $\rho = T^2\sigma_A^2$ which simplifies the expressions to follow [14]. Based on the above definitions and normalizations, the PDF of x_s conditioned on H_0 and H_1 is

$$x_s \sim \begin{cases} \text{CN}(0, 1 + \rho), & \text{under } H_1, \\ \text{CN}(0, 1), & \text{under } H_0. \end{cases} \quad (4)$$

Consequently, the PDF of z_s defined in (2) conditioned on H_0 and H_1 is Chi-Squared central with two degrees of freedom (DOF). (If $B \sim \text{CN}(0, \sigma^2)$, $|B|^2$ is distributed according to $f(|B|^2) = 1/\sigma^2 \exp(-|B|^2/\sigma^2)$.)

Hence [17],

$$z_s \sim \begin{cases} e^{-z_0}, & \text{under } H_0, \\ \frac{1}{\rho + 1} e^{-(z_0/(\rho+1))}, & \text{under } H_1. \end{cases} \quad (5)$$

Assuming that z_s is compared with a threshold γ , then the P_{fa} and P_d can be determined by [17]

$$\begin{aligned} P_{fa} &= \exp(-\gamma), \\ P_d &= \exp\left(\frac{-\gamma}{1 + \rho}\right). \end{aligned} \quad (6)$$

Let ρ_s denote the value of ρ for the static antenna that can be expressed explicitly in terms of the given target values of P_{fa} and P_d using (6) as

$$\rho_s = \frac{\ln(P_{fa})}{\ln(P_d)} - 1. \quad (7)$$

ρ_s is the average SNR required to meet the target values of P_{fa} and P_d for a static antenna assuming Rayleigh fading.

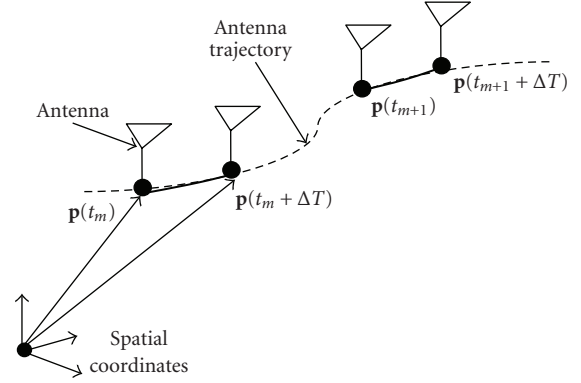


FIGURE 1: Synthetic array model illustrating signal collection over the m th and $(m + 1)$ th subintervals.

3. Synthetic Array System Model and Detection Performance

The synthetic array antenna is now considered where the single antenna is moving along an arbitrary trajectory while the snapshot data is being collected. The position vector to the antenna location at time t from the origin is now denoted as $\mathbf{p}(t)$. The signal component of the complex baseband signal $r(t)$ is written as $s(t, \mathbf{p}(t))$, which is a function of time, t , and the antenna position, $\mathbf{p}(t)$, which in turn is a function of t . The signal is assumed to be narrowband implying that the reciprocal of the maximum delay extent of the antenna trajectory is much larger than the bandwidth of $s_0(t)$. The signal bandwidth is also small relative to the coherence bandwidth of the propagation channel. Figure 1 illustrates a realization of the synthetic array antenna with an arbitrary trajectory. During the antenna movement, the receiver collects M spatial samples, each with coherent integration intervals of ΔT . Note that the M spatial samples are taken sequentially.

The narrowband assumption justifies the decomposition of $s(t, \mathbf{p}(t)) = A(\mathbf{p}(t))s_0(t)$, which implies that the small delay changes due to $\mathbf{p}(t)$ are insignificant in the context of $s_0(t)$. It is assumed that the signal snapshot of $r(t)$ is collected in M subintervals, each of duration ΔT . The constraint $T = M\Delta T$ is imposed such that the static antenna and synthetic array antenna can be compared directly. Define t_m as the starting instance of the m th subinterval that extends over the interval of $[t_m, t_m + \Delta T]$ for $m \in [1, 2, \dots, M]$. It is assumed that there can be arbitrary time gaps between the subintervals such that $t_m - t_{m-1} > \Delta T$. The collection of signal over the m th and $(m + 1)$ th subintervals is illustrated in Figure 1.

As stated earlier, ΔT is considered to be sufficiently small such that $A(\mathbf{p}(t))$ can be approximated as constant over the subinterval of ΔT . The signal captured in each subinterval is correlated with $s_0(t)$ resulting in a set of M spatial array samples denoted by x_m and given as

$$x_m = \frac{1}{\Delta T} \int_{t_m}^{t_m + \Delta T} r(t) s_0(t)^* dt. \quad (8)$$

x_m is expressed as

$$x_m = A(\mathbf{p}(t_m))s_m + w_m, \quad (9)$$

where

$$\begin{aligned} s_m &= \frac{1}{\Delta T} \int_{t_m}^{t_m+\Delta T} |s_0(t)|^2 dt, \\ w_m &= \frac{1}{\Delta T} \int_{t_m}^{t_m+\Delta T} w(t)s_0(t)^* dt. \end{aligned} \quad (10)$$

Based on these assumptions made, it follows that x_m forms a set of sufficient statistics of the accumulated snapshot signal in terms of optimal decoding between H_0 and H_1 . The vector forms of the signals are defined as $\mathbf{x} = [x_1, \dots, x_M]^T$, $\mathbf{s} = [s_1, \dots, s_M]^T$, $\mathbf{w} = [w_1, \dots, w_M]^T$, and $\mathbf{A} = [A(\mathbf{p}(t_1)), \dots, A(\mathbf{p}(t_M))]^T$. With these definitions the detection problem is stated as [14]

$$\begin{aligned} \mathbf{x}|_{H_1} &= \mathbf{A} \odot \mathbf{s} + \mathbf{w}, \\ \mathbf{x}|_{H_0} &= \mathbf{w}, \end{aligned} \quad (11)$$

where \odot denotes the Hadamard vector product operator. The noise covariance matrix is denoted as \mathbf{C}_w and given as

$$\mathbf{C}_w = E[\mathbf{w}\mathbf{w}^H] = \frac{1}{M} \mathbf{I}_M, \quad (12)$$

where \mathbf{I}_M is an $M \times M$ identity matrix. The last step follows from the normalization $TN_o = 1$ and that $\int_{t_m}^{t_m+\Delta T} |s_0(t)|^2 dt \approx T/M = \Delta T$, which is based on the assumption that the bandwidth of the spreading signal $s_0(t)$ is much larger than $1/\Delta T$. The signal covariance matrix is denoted as \mathbf{C}_s and given as

$$\mathbf{C}_s = E[\mathbf{A} \odot \mathbf{s}(\mathbf{A} \odot \mathbf{s})^H] = \Delta T^2 \mathbf{C}_A, \quad (13)$$

where \mathbf{C}_A is the covariance matrix of \mathbf{A} . As stated previously, the individual components of the vector \mathbf{A} are circularly normal such that $[\mathbf{A}]_m = A(\mathbf{p}(t_m)) \sim \text{CN}(0, \sigma_A^2)$. The signal covariance matrix in a Rayleigh fading environment with ring of scatterer models can be defined by [20]

$$\begin{aligned} \mathbf{C}_s &\approx \frac{\sigma_A^2 T^2}{M^2} \Psi = \frac{\rho}{M^2} \Psi, \\ [\Psi]_{i,j} &= J_0\left(\frac{2\pi}{\kappa} |\mathbf{p}_i - \mathbf{p}_j|\right), \end{aligned} \quad (14)$$

where Ψ denotes normalized correlation coefficient matrix which is a function of antenna position, J_0 is zero-order Bessel function of the first kind, and κ is the carrier wavelength. Based on (12) and (14), the PDF of \mathbf{x} conditioned on H_1 and H_0 is

$$\mathbf{x} \sim \begin{cases} \text{CN}(0, \mathbf{C}_s + \sigma_w^2 \mathbf{I}) = \text{CN}\left(0, \frac{\rho}{M^2} \Psi + \frac{1}{M} \mathbf{I}\right) & \text{under } H_1, \\ \text{CN}(0, \sigma_w^2 \mathbf{I}) = \text{CN}\left(0, \frac{1}{M} \mathbf{I}\right) & \text{under } H_0. \end{cases} \quad (15)$$

3.1. Optimum Detection Performance of a Narrowband Signal in Rayleigh Fading. The optimal detection processing based on the likelihood Ratio Test (LRT) chooses H_1 if [17]

$$L(\mathbf{x}) = \frac{p(\mathbf{x}|_{H_1})}{p(\mathbf{x}|_{H_0})} > \gamma, \quad (16)$$

where $p(\mathbf{x}|_{H_1})$ and $p(\mathbf{x}|_{H_0})$ are the conditional PDF's of \mathbf{x} given H_1 and H_0 , respectively. As both \mathbf{A} and \mathbf{w} are zero mean multivariate Circular Gaussian random vectors, so is \mathbf{x} . Hence, $L(\mathbf{x})$ is a function of the covariance matrices of $\mathbf{A} \odot \mathbf{s}$ and \mathbf{w} .

After some manipulation and removing deterministic scaling and additive constants, the LRT reduces to the Estimator-Correlator (EC) formulation [19] resulting in a sufficient statistic given as

$$z_{\text{EC}}(\mathbf{x}) = \mathbf{x}^H \mathbf{C}_s (\mathbf{C}_s + \sigma_w^2 \mathbf{I})^{-1} \mathbf{x}, \quad (17)$$

where σ_w^2 and \mathbf{C}_s are defined in (15). Since \mathbf{C}_s is a Hermitian matrix, the eigen-decomposition of \mathbf{C}_s can be represented as

$$\mathbf{V}^H \mathbf{C}_s \mathbf{V} = \Lambda_s, \quad (18)$$

where $\mathbf{V} = [\mathbf{v}_1 \mathbf{v}_2 \dots \mathbf{v}_M]$ is the orthogonal matrix of columnwise eigenvectors and Λ_s is the diagonal matrix of eigenvalues where the m th eigenvalue is denoted by λ_{s_m} . The test statistics in (17) can be shown as [17]

$$z_{\text{EC}}(\mathbf{y}) = \sum_{m=1}^M \frac{\lambda_{s_m}}{\lambda_{s_m} + \sigma_w^2} |y_m|^2, \quad (19)$$

where $\mathbf{y} = \mathbf{V}^H \mathbf{x}$. The vector $\mathbf{y} = [y_1, y_2, \dots, y_M]^T$ consists of M independent circular Gaussian random variables such that [17]

$$\mathbf{y} \sim \begin{cases} \text{CN}\left(0, \Lambda_s + \frac{\mathbf{I}}{M}\right) & \text{under } H_1, \\ \text{CN}\left(0, \frac{\mathbf{I}}{M}\right) & \text{under } H_0. \end{cases} \quad (20)$$

Therefore, the test statistics, z_{EC} becomes a scaled factor of Chi-Squared distribution. Figure 2 shows the synthetic array processing model and the canonical form of the EC process.

Next consider the calculation of the P_{fa} and P_d . The characteristic function of z_{EC} conditioned on H_1 and H_0 is given as [19]

$$\begin{aligned} \phi_{z|_{H_1}}(\omega) &= \prod_{m=1}^M \frac{1}{1 - j\alpha_m^{H_1} \omega}, \\ \phi_{z|_{H_0}}(\omega) &= \prod_{m=1}^M \frac{1}{1 - j\alpha_m^{H_0} \omega}, \end{aligned} \quad (21)$$

where

$$\begin{aligned} \alpha_m^{H_1} &= \lambda_{s_m}, \\ \alpha_m^{H_0} &= \frac{\lambda_{s_m}}{M\lambda_{s_m} + 1}, \end{aligned} \quad (22)$$

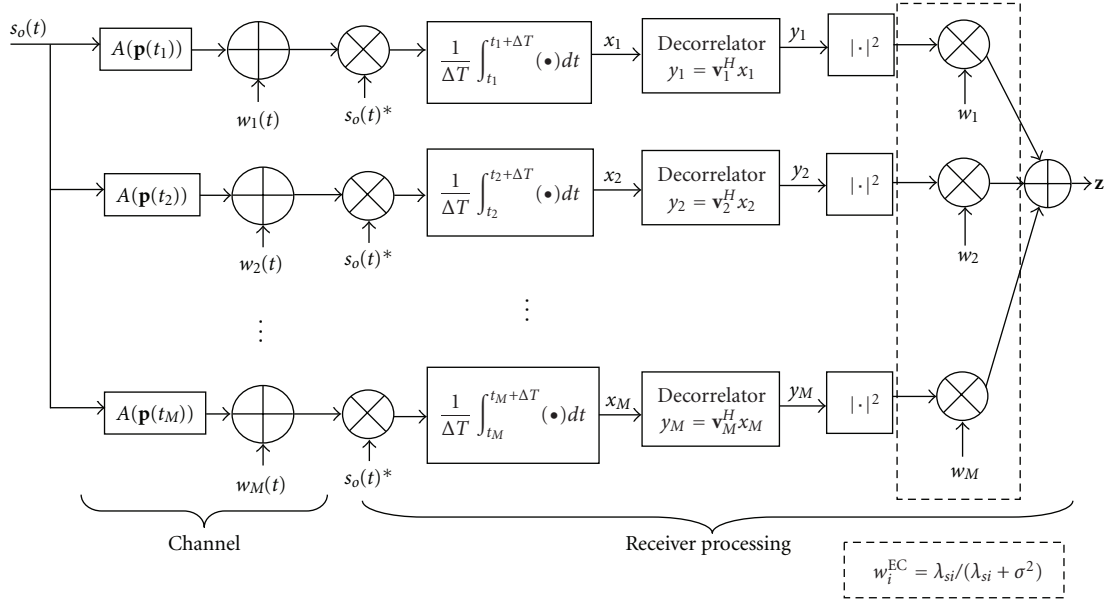


FIGURE 2: Synthetic antenna channel model and subsequent EC processing.

The values of P_{fa} and P_d can be determined by taking the Fourier transform of the characteristic functions [17]. For a given threshold of γ applied to z_{EG} , the following is obtained:

$$P_d = \int_{\gamma}^{\infty} \int_{-\infty}^{\infty} \phi_{z|H_1}(\omega) e^{-j\omega z} \frac{d\omega}{2\pi} dz, \quad (23)$$

$$P_{fa} = \int_{\gamma}^{\infty} \int_{-\infty}^{\infty} \phi_{z|H_0}(\omega) e^{-j\omega z} \frac{d\omega}{2\pi} dz.$$

A closed form expression for P_{fa} and P_d in case of distinctive eigenvalues of \mathbf{C}_s is given in the appendix.

3.2. Detection Performance of the Equal Gain (EG) Combiner in Rayleigh Fading. As it is shown in (19) the EC emphasizes the stronger signal components corresponding to those with the larger eigenvalues. EC formulation requires approximate knowledge of signal and noise covariance matrices in order to compute the eigenvalues. This may not be applicable in many practical applications. When \mathbf{C}_w and \mathbf{C}_s are not known *a priori*, the EG combiner is a practical suboptimal alternative that may be applied. Note from (19) that the EG combiner becomes asymptotically optimal when the signal becomes more uncorrelated. On the other hand, EG combiner is an optimal approach for signal detection in uncorrelated Rayleigh fading channels. This is because $\lambda_{s_m}/(\lambda_{s_m} + \sigma_w^2)$ in (19) becomes identical for all spatial samples that leads to EG formulation. The test statistics of EG combiner can be represented by [6]

$$z_{EG} = \mathbf{x}^H \mathbf{x} = \sum_{m=1}^M |x_m|^2. \quad (24)$$

As it is shown in (24) the test statistics of EG combiner is independent of \mathbf{C}_s . To determine the performance of EG in correlated Rayleigh fading, it is convenient to perform

the following transformation, which decorrelates the signal covariance matrix [17]:

$$z_{EG} = \mathbf{x}^H \mathbf{x} = \mathbf{x}^H \mathbf{V} \mathbf{V}^H \mathbf{x}$$

$$= \mathbf{y}^H \mathbf{y} = \sum_{m=1}^M |y_m|^2, \quad (25)$$

with $\mathbf{y} = \mathbf{V}^H \mathbf{x}$ where \mathbf{V} is the eigenvectors of signal covariance matrix defined earlier. The distribution of \mathbf{y} is given in (20). Consequently

$$y_m \sim \text{CN}(0, \lambda_m^{H_i}), \quad i = 0, 1, \quad (26)$$

$$|y_m|^2 \sim \frac{1}{\lambda_m^{H_i}} \chi_2^2 \left(\frac{z}{\lambda_m^{H_i}} \right),$$

where $\lambda_m^{H_i}$ is the m th eigenvalue of \mathbf{C}_s under H_i state and χ_2^2 denotes Chi-Squared distribution with two DOF. For a general signal covariance matrix \mathbf{C}_s , the characteristic function of z_{EG} conditioned on H_1 and H_0 is given as

$$\phi_{z|H_1}(\omega) = \prod_{m=1}^M \frac{1}{1 - j\lambda_m^{H_1} \omega}, \quad (27)$$

$$\phi_{z|H_0}(\omega) = \prod_{m=1}^M \frac{1}{1 - j\lambda_m^{H_0} \omega},$$

where

$$\lambda_m^{H_1} = \lambda_{s_m} + \frac{1}{M}, \quad (28)$$

$$\lambda_m^{H_0} = \frac{1}{M}.$$

The values of P_{fa} and P_d can be determined by inserting (27) into (23).

In summary the following points are made.

- (i) In a correlated signal environment, the optimum detector for a signal in Gaussian noise is the EC, for which the test statistic is given in (19). This procedure requires *a priori* knowledge of the covariance matrix and signal power. The EC performances were determined by inserting (21) into (23). The closed form expressions of EC performance for distinctive eigenvalues of signal covariance matrix is given in the appendix.
- (ii) When the multipath fading is such that the channel gains associated with the M samples of the synthetic array become uncorrelated, then the EC process reduces to the EG combiner. In this case, the test statistic becomes a random variable with a central Chi-squared PDF with $2M$ DOF.
- (iii) When the multipath fading is such that the channel gains associated with the M samples of the synthetic array become fully correlated, then the EC combining reduces to that of a matched filter followed by a magnitude squaring operation. In this case, the test statistic is random with a central Chi-square PDF of two DOF. The test statistic and performance are therefore equivalent to that of the static antenna as represented in (2) and (6).
- (iv) When C_s and C_w are unknown, a suboptimal solution is provided by the EG combiner. The performances of the EG combiner in correlated Rayleigh fading were demonstrated by inserting (27) into (23).

4. Analysis of Processing Gains and Practical Implementation Issues

In this section, the detection performances of a receiver using a static antenna and a synthetic array are compared for a Rayleigh multipath fading. The EG and EC combiners are considered for the synthetic array. The covariance matrix of the signal samples C_s is assumed to be known. The performance comparison of the static antenna and synthetic array antenna receivers will be achieved by the following approach.

- (i) Assume fixed target values for P_{fa} and P_d
- (ii) Determine the average SNR ρ required to meet these target objectives. These will be denoted as ρ_s , ρ_{EG} , and ρ_{EC} for the static antenna, synthetic array with EG combining, and synthetic array with EC combining, respectively.
- (iii) The performance advantage of the synthetic array with EG or EC combining relative to the single static antenna is then given as $G_{EG} = 10 \log(\rho_s/\rho_{EG})$, $G_{EC} = 10 \log(\rho_s/\rho_{EC})$, respectively.

While the formulation presented thus far is for an arbitrary number of samples M of the synthetic array, the

special case of $M = 2$ is considered in detail as this is compatible with the experimental results given in Section 5. For $M = 2$, using (14), the signal covariance matrix is given as

$$C_s = \frac{\rho}{4} \begin{bmatrix} 1 & r \\ r & 1 \end{bmatrix}, \quad (29)$$

where r is the correlation coefficient which is a function of antenna spacing.

The left column of Figure 3 shows the average SNR required to achieve different target values of p_{fa} and p_d given the correlation coefficient r which varies between zero and one. The right column of Figure 3 also reveals the corresponding gain of the synthetic array processing schemes, G_{EC} and G_{EG} , from which several significant observations can be made. The required average SNR for a single antenna is significantly higher than that of the synthetic array schemes. For the uncorrelated case, $r = 0$, the gain is about 4 dB for $p_{fa} = 0.05$ and $p_d = 0.95$. This is essentially a result of the diversity gain possible. Note that there is no suppression of the channel noise for the dual antenna schemes possible when $r = 0$ as the signal samples emerging from the antennas are uncorrelated. Hence, the observed gain corresponding to $r = 0$ is strictly diversity gain. When r approaches one, the signal components emanating from the pair of antennas are correlated and hence there is no diversity gain. In this case, there is identical gain on the EC scheme with a static antenna. This is a result of the averaging of the pair of uncorrelated noise samples due to the coherent combining of the EC. When high system performance is required, there is a negligible advantage of the EC processing over the EG processing for realistically encountered values of the correlation coefficient. This phenomenon is shown in Figures 3(a) and 3(b). Only when r is close to one, there is an advantage in using EC over EG. This has a practical significance in that the parameters ρ and r do not have to be estimated by the receiver. By decreasing the probability of detection and increasing the probability of false alarm the advantage of using EC becomes more evident. As it is shown in Figures 3(c), 3(d), 3(e), and 3(f), the achievable gain from EC and EG is identical only when the correlation coefficient r is less than 0.8 and 0.7, respectively, for ($P_{fa} = 0.1$ $P_d = 0.9$) and ($P_{fa} = 0.15$ $P_d = 0.85$).

Figure 3 demonstrated that the performance of the synthetic array with the EC process is better or identical to that of the static antenna for all range of r . Although the performances of the EG and EC combiners are almost indistinguishable for correlated cases with r values of up to about 0.75, in highly correlated situations the performance of the EG combiner becomes worse than that of the static antenna which means that there is performance loss when moving the antenna. This happens when the processing gain of EG combiner shown in Figure 3 goes below zero dB. Thus, it is investigative to determine values of r for which zero crossing occurs. Figure 4 shows values of correlation coefficient for a range of target detection performance metrics $\{P_d, P_{fa}\}$ for which the detection performance of the synthetic array based on the EG combiner becomes worse

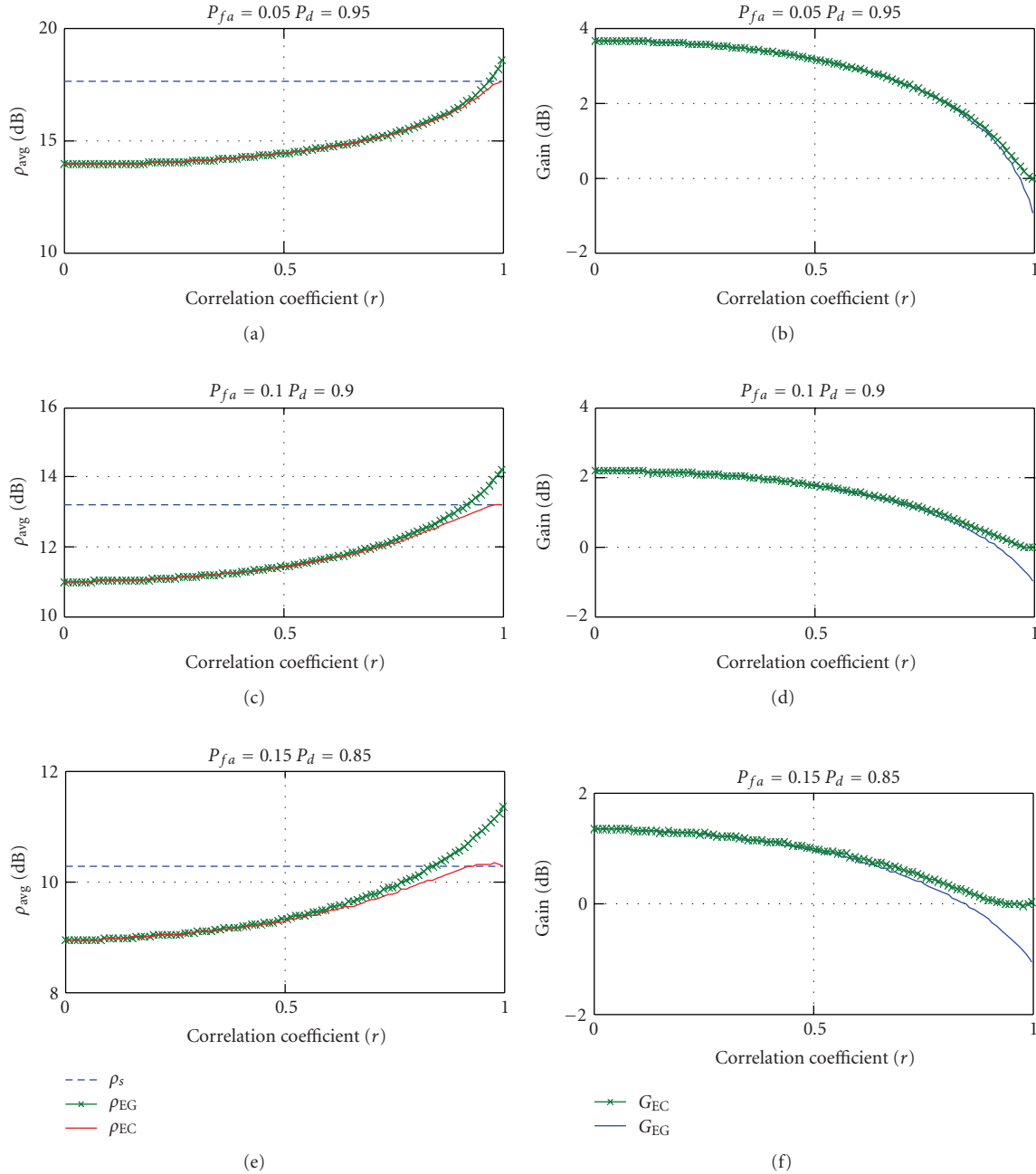


FIGURE 3: (a), (c), and (e) required SNR for the stationary and synthetic antenna with EC and EG for target values of P_{fa} and P_d ; (b), (d), and (f) processing gain of synthetic array with EC and EG combiner.

than that of the static antenna. By requiring higher detection performance, the zero crossing occurs in higher values of correlation coefficient. As an example when $P_d = 0.99$ and $P_{fa} = 0.01$, the zero crossing happens at $r = 0.98$, however for $P_d = 0.8$ and $P_{fa} = 0.1$ zero crossing occurs at $r = 0.8$. Figure 4 shows upper boundaries of correlation coefficient values for which the EG combiner provides diversity gain with respect to the static antenna. Resulting from Figure 4, if the correlation coefficient value is less than 0.8, the synthetic array based on the EG combiner has diversity gain over the static antenna. To satisfy this condition in a Rayleigh fading

environment with the ring of scatterers model, pairwise antenna spacing must be greater than 0.15 of the carrier wavelength.

The receiver operating characteristics (ROCs) curves, which are plots of P_d as a function of P_{fa} for specific value of ρ , are commonly used to demonstrate the performance of a receiver. Figure 5 represents ROC curves versus r for given values of SNR (16 dB) and $M = 2$. By increasing the correlation coefficient r , the performance reduction due to correlation becomes more apparent. As expected in moderate correlated cases ($r < 0.75$) performance of EC and

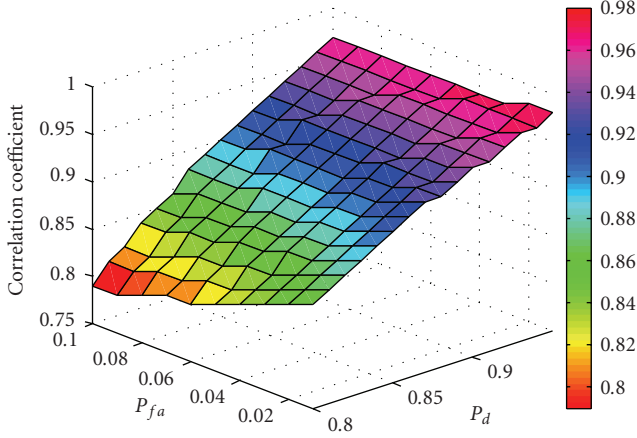


FIGURE 4: Values of correlation coefficient where the performance of EG combiner becomes worse than static antenna for a range of target detection performance metrics.

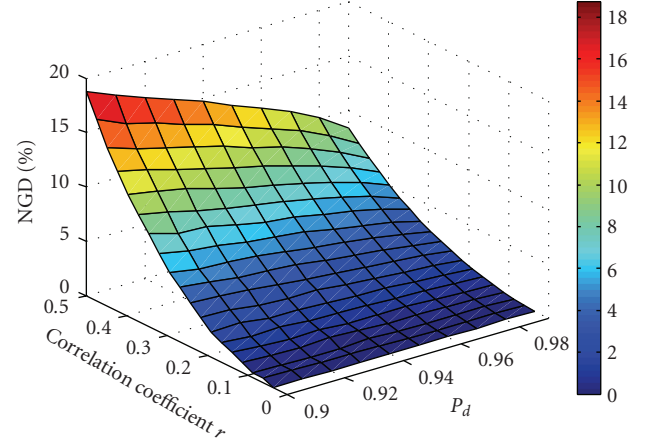


FIGURE 6: NGD for different values of correlation coefficient and P_d for $P_{fa} = 0.05$.

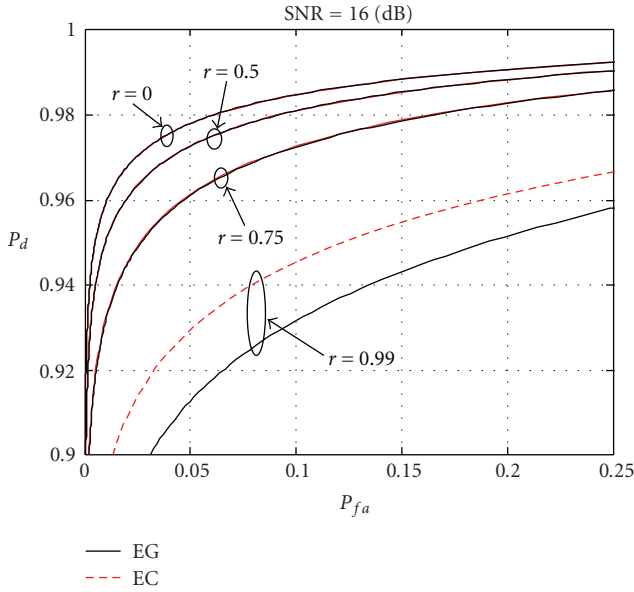


FIGURE 5: ROC curves for given SNR and r .

EG is identical. Figure 5 also shows ROC curves for almost coherent case where $r = 0.99$. In this case the performance of EC is superior to that of the EG.

An important implementation factor of the synthetic array is estimating the trajectory of the moving antenna to capture statically independent spatial samples. As it is shown in (14) the signal covariance matrix \mathbf{C}_s depends only on pair wise distance between spatial sampling points, denoted here as d , which is determined by the approximate velocity and time interval between samples taken by a moving antenna. Thus, no matter the array shape and configuration, as long as any pairs of spatial samples have appropriate spacing, diversity gain are attainable. This resolves the problem of precise trajectory estimation and array calibration, which are practical implementation difficulties associated with

beamforming techniques [12, 20]. However, in practice the receiver requires a rough estimate of the motion velocity such that it can reject highly correlated samples due to insufficient spatial separation. This can be accomplished by implementing a consumer grade accelerometer devices which only needs to estimate the spatial distance between samples [13].

To analyze the sensitivity of the proposed method to a trajectory estimation error, a scenario with two antenna positions is considered. The problem of interest is determining the degradation in processing gain of the synthetic array due to a trajectory estimation error. Since the signal correlation matrix is a function of antenna spacing, considering some errors in the trajectory estimation unit, the processed spatial samples may become correlated. Hence, the EG detector is no longer the optimum process. However, the EG combiner has numerous implementation benefits and it is preferred for implementation in practice. The performances of the EC and the EG combiner for different correlation coefficient values of the Rayleigh channel are compared in Figures 3 and 5, and it was shown for moderate correlation coefficient that the EG combiner is a practical option.

Normalized gain degradation (NGD) can be defined as a designing metric to quantify the performance degradation of a diversity system due to correlated fading. NGD is defined by the percentage of the diversity gain difference between uncorrelated and correlated processes normalized by the diversity gain in the uncorrelated case:

$$\text{NGD} = \left(\frac{G_{\text{EG}}^{r=0} - G_{\text{EG}}^{r=q}}{G_{\text{EG}}^{r=0}} \right) \times 100, \quad q \in [0, 1], \quad (30)$$

where $G_{\text{EG}}^{r=0}$ is the EG combiner processing gain for uncorrelated case.

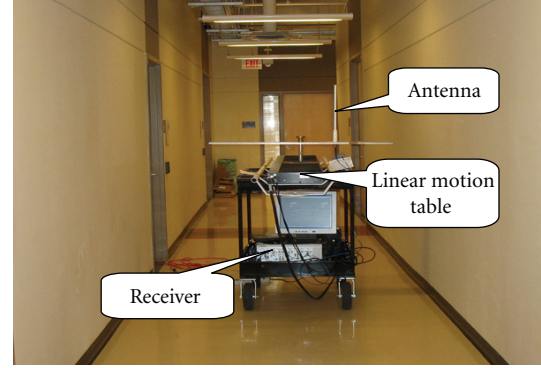
Figure 6 shows NGD for desired range of P_d and correlation coefficient values. As expected, increasing r results in performance degradation. This performance reduction is

more severe for low values of P_d . Figure 6 also gives a designing perspective regarding the performance degradation. As an example if a synthetic array diversity system must work within 10% of the maximum diversity gain, the amount of the correlation coefficient, which the diversity system can tolerate, is extracted directly from Figure 6. For nominal detection performances of $P_d = 0.98$, to have NGD value within 10 percent, the correlation coefficient should be less than 0.45 which means that based on the ring of scatters model the antenna spacing should be more than quarter of the carrier wavelength. Hence, by appropriate design of the unit trajectory estimation, the gain degradation due to a trajectory estimation error can be removed.

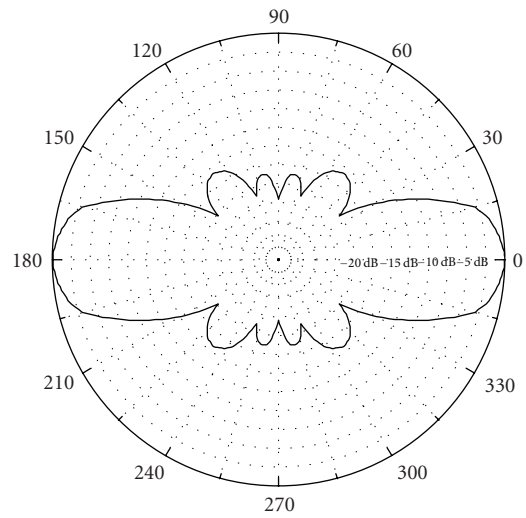
5. Experimental Results

In the previous sections, the theoretical gain of the synthetic array was determined based on the Rayleigh fading model with the assumption that the channel gain, $A(\mathbf{p})$, is a circular normal random process with respect to the antenna position \mathbf{p} but temporally static with respect to the snapshot interval. This led to usable expressions for the relative processing gain. It is shown that the processing gain due to synthetic array processing diminishes with increasing correlation coefficient, the latter being a function of antenna spacing and diffuse multipath characteristics. It was also shown that the performance of the optimal EC is almost the same as the performance of the suboptimal EG combiner in cases where the channel gain is moderately correlated. In this section the EG combiner is utilized to validate the theoretical achievements represented in the previous sections. The experimental measurements described in this section attempt to partially validate the application of these assumptions in the context of the synthetic array for indoor environments. The objective of the experimental measurements is to determine processing gain for a selection of typical indoor locations and compare these with corresponding theoretical values. Experimental measurements involving indoor multipath scenarios are generally plagued with the issue of attaining statistical significance.

The experimental measurements are based on the indoor reception of a terrestrial CDMA-2000 pilot signal emanating from an outdoor base station located about 1 km from the indoor location. The pilot channel has no data modulation and consists of only in-phase and quadrature phase pseudonoise (PN) codes. All BSs use the same PN code, distinguished by the different code offsets. The receiver is tuned to capture CDMA signals with a bandwidth of 1.25 MHz modulated by 1.2288 Mchip/s PN sequence with the period of 2^{15} chips at 1947.5 MHz [21]. Signals received at the antennas are amplified, filtered, down-converted, and sampled by 10 MHz digitizer board. The detection process in this case can be formulated as a binary multihypothesis test problem where the objective is to determine the correct code phase between received and replica signals and discarding all incorrect code phases under the constraint of a tolerable rate of false detections. The condition where the code phase of the locally generated despreading signal is different from



(a)



(b)

FIGURE 7: (a) Data collection environment and measurement equipment. (b) Vertical pattern of the antenna.

that of the incoming signal corresponds to the H_0 state where equivalently there is no discernable signal. In this state the p_{fa} can be evaluated. Likewise, if the code phase of the locally generated despreading signal is the same as that of the incoming signal, then it corresponds to an H_1 state where the signal is present from which the p_d can be evaluated. A vertically polarized omnidirectional antenna in horizontal plane was mounted on the linear motion table to capture the CDMA pilot signals. Figure 7 shows a photograph of the data collection environment and measurement equipment used and vertical antenna pattern. The theoretical findings represented in the previous sections were based on the ring of scatterers model which reduced to a signal correlation matrix represented in (14). Although, in general, indoor propagation model may be characterized by a sphere of scatterers model, due to vertical pattern of the antenna shown in Figure 7 the scatterers geometry can be approximately characterized by a ring model.

As mentioned earlier, the diversity gain results as an effect of the independency of spatially separated samples.

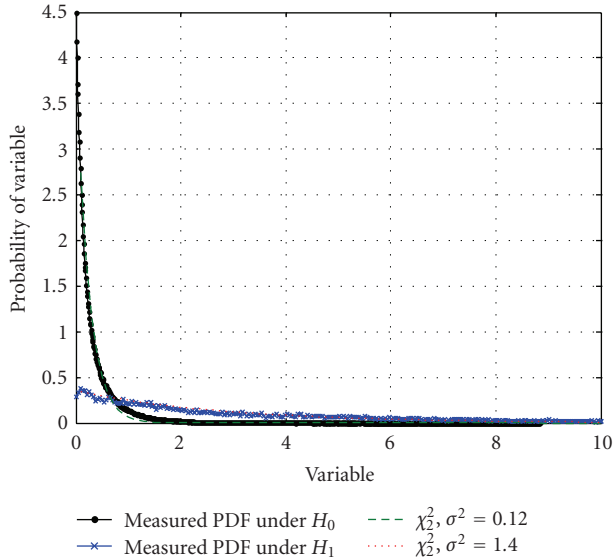


FIGURE 8: Numerically calculated PDF under H_0 and H_1 states for a static antenna.

Therefore, it is essential to evaluate the channel spatial correlation coefficients. To this end, the spatial covariance matrix is estimated based on all spatial samples on the linear moving table. The measurement results agree fairly well with the theoretical model of ring of scatterers defined in (14). Thus, based on the measurement results, arrival signals onto two spatial samples separated by half of a wavelength are approximately uncorrelated.

The second set of experimental measurements was aimed at producing ROC curves. The results obtained for the static antenna and synthetic array for different antenna correlations, a process controlled by choosing different antenna spacings, were then compared with calculations based on the theoretical expressions for P_d and P_{fa} derived earlier. The spatial samples were taken while the antenna was moving at constant speed with a velocity of 0.2 m/s. To evaluate the detection performance of a moving antenna, comprehensive data collections shown in Figure 7 at various locations in the hallway were collected and the conditional PDFs corresponding to the H_0 and H_1 states were numerically calculated based on the measured sample set. Figure 8 shows the measured PDFs of test statistics z_s under H_0 and H_1 for static antenna. For comparison, the PDFs of Chi-Squared central distributions with two DOFs (χ_2^2) are overlaid. Figure 9 shows measured and theoretical PDFs of test statistics for the moving antenna (z_{EG}) under H_0 and H_1 when $M = 2$ and $d = \kappa/2$ where κ is the carrier wavelength. The theoretical PDFs in Figure 9 are Chi-Squared central distributions with four DOFs (χ_4^2). The match with the theoretical Chi-Squared density functions, which results from the uncorrelated Rayleigh fading assumption, is reasonable and verifies the validity of the Rayleigh fading model.

Based on the fitting to the Chi-Squared PDFs of Figures 8 and 9 results of (15), it can be shown that $\sigma^2_{H_1}/\sigma^2_{H_0} = ((\rho/M) + 1)$. Hence, the average SNR and ρ can be extracted

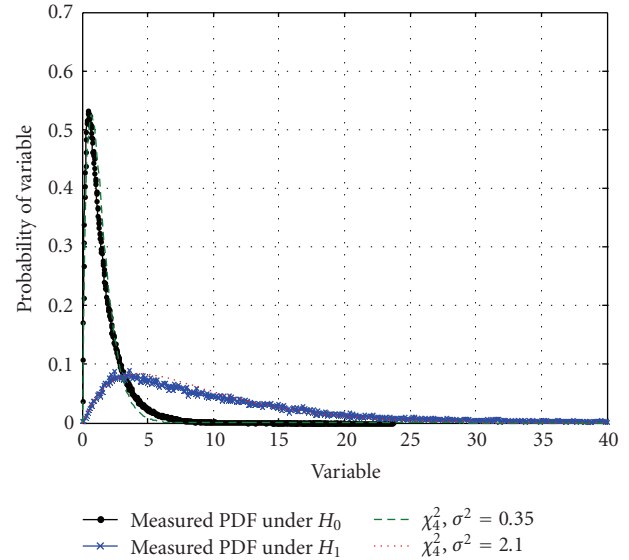


FIGURE 9: Numerically calculated PDF under H_0 and H_1 states for a moving antenna.

from the overlaid theoretical PDFs. Based on measurement results, for static and moving antennas, the average SNRs are approximately $\rho_s = 10.2$ dB and $\rho_{EG} = 10$ dB, respectively. Figure 10 shows numerically calculated ROC curves based on measurements for the synthetic array and static antenna. The detection performance of the synthetic array with two statistically uncorrelated sensors is significantly better than that of the static antenna. To determine the synthetic array gain over the static antenna in term of required average SNR, the measured ROC curves of a synthetic array with average SNR of $\rho_{EG} = 8.6$ dB are also plotted in Figure 10, which fits to the ROC curves of the static antenna. The average SNR is decreased by adding noise to the process. From this, the synthetic array gain over static antenna can be obtained and is about $G_{EG} = 1.6$ dB. The target performance of $p_{fa} = 0.15$ and $p_d = 0.85$ is nearly located on the ROC curve of the static antenna, as shown in Figure 10. The theoretical gain of the synthetic array with target values of $p_{fa} = 0.15$ and $p_d = 0.85$ was shown in Figures 3(e) and 3(f). The theoretical gain for the uncorrelated case ($r = 0$) is about 1.6 dB, which matches fairly well with the measurements results.

Figure 11 shows measured PDFs for the synthetic antenna array under H_1 state for different antenna spacings d in terms of carrier wavelength κ . Figure 11 shows that, by decreasing antenna spacing or increasing the correlation coefficient, the mean value of the detection variable decreases. This phenomenon causes losing the diversity gain. Figure 11 also shows that, by increasing the correlation coefficient, the test statistics PDFs moves from a central Chi-Squared with four DOFs χ_4^2 toward a central Chi-Squared with two DOFs χ_2^2 , which again results in a lower diversity gain. Another observation is that the measured PDFs fits fairly well with theoretical PDFs for the different correlation coefficients and antenna spacings derived in (26).

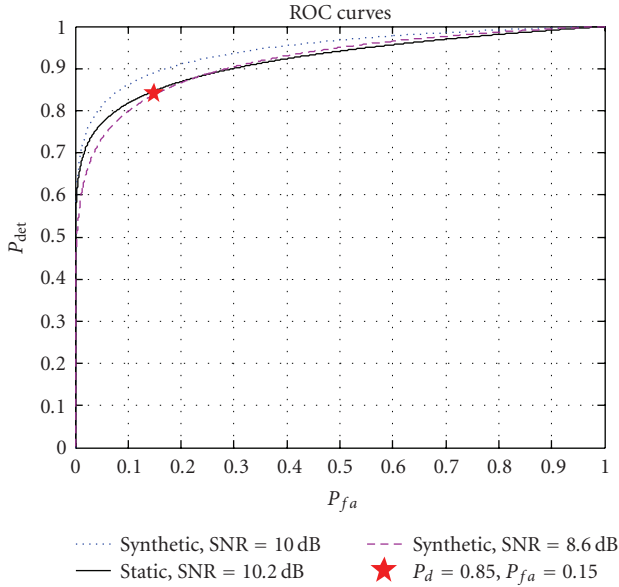


FIGURE 10: Numerically calculated ROC curves in an uncorrelated case.

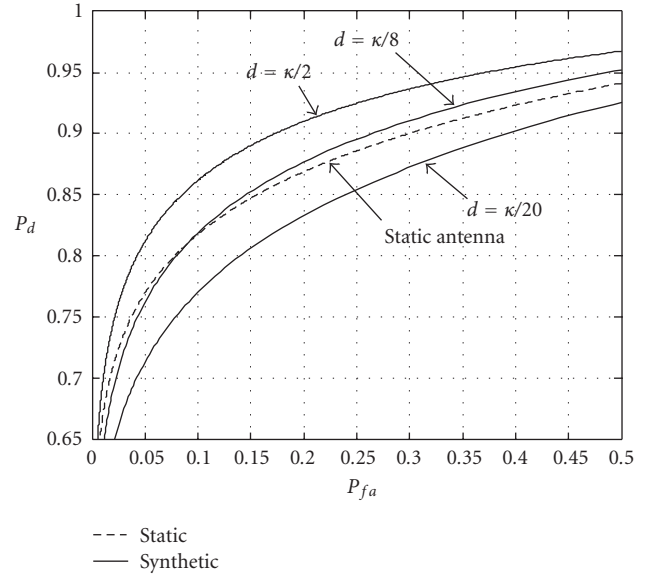


FIGURE 12: Measured ROC curves for static antenna and synthetic array.

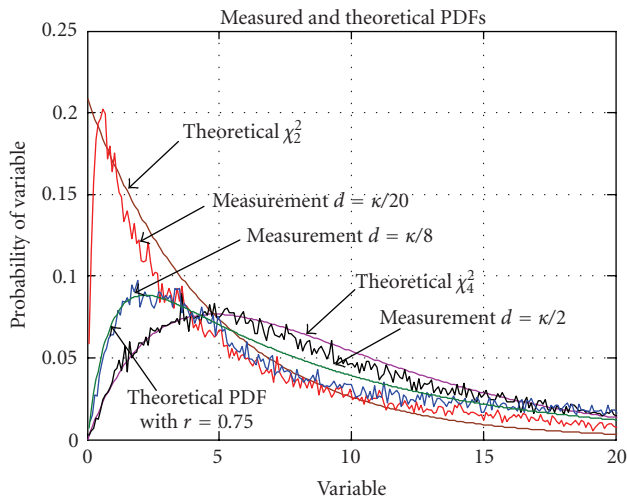


FIGURE 11: PDFs of the synthetic array under H_1 state for different antenna spacings.

Figure 12 shows ROC curves obtained with different synthetic antenna spacings d . The corresponding ROC curves for the static antenna are generated in a similar manner based on coherent summations of stationary samples and are also shown in the figure. As expected the synthetic antenna with a synthetic element spacing of $\kappa/2$ with approximately uncorrelated samples outperforms all other scenarios. Figure 12 shows that, by decreasing antenna spacing, the performance of the EG combiner degrades due to the correlated signal covariance matrix. It is also shown that the performance of the coherent integration in the static case is almost the same as that of the synthetic antenna array with a spacing of $\kappa/8$ which can be directly compared

with the theoretical results of Figure 4. By decreasing the antenna spacing to $\kappa/20$, the performance worsens, which demonstrates that there is no advantage of using a synthetic array.

6. Conclusions

The performance enhancement of a synthetic antenna array as compared to a static antenna subjected to a correlated Rayleigh fading environment was demonstrated. A synthetic array of two antennas was selected for a direct comparison of experimental results with theoretical expectations. It was shown that, in such fading environments, a synthetic antenna with two elements for practical target performance values provides a net gain advantage of 4 dB, which is comprised essentially of diversity gain. More spatial samples would provide further gains due to further diversity gains. If the correlation of the signal samples is increased, then the diversity gain diminishes eventually to the point where the moving antenna has no advantage over the static antenna. Of interest was the determination of the performance degradation of the EG combiner due to the correlation with respect to an optimal EC approach. The results show that in moderate correlation environments, the performance of EC and EG combiners is almost identical. Experimental measurements were performed to verify the assumption of the Rayleigh fading and also to confirm the theoretical processing gain. A reasonable agreement between the experimental and theoretical results was observed.

The assumption utilized herein was based on the flat Rayleigh fading where there is not a well-defined LOS signal component and the signal bandwidth is much smaller than

the coherence bandwidth of the channel. The results presented herein may be generalized by considering the presence of the LOS signal and resolvable multipath components. In addition, the synthetic array concept presented in this paper may be considered for other antenna diversity systems and combining methods.

Appendix

Closed Form Expression for P_{fa} and P_d in Case of Distinctive Eigenvalues of the EC Process

To determine a closed form expression for P_{fa} and P_d in case of distinctive eigenvalues of \mathbf{C}_s , using a partial fraction expansion, it can be shown that [17]

$$\prod_{m=1}^M \frac{1}{1 - j\alpha_m^{H_i} \omega} = \sum_{m=1}^M \frac{A_m^{H_i}}{1 - j\alpha_m^{H_i} \omega}, \quad i = 0, 1, \quad (\text{A.1})$$

where

$$A_m^{H_i} = \prod_{\substack{k=1 \\ k \neq m}}^M \frac{1}{1 - (\alpha_k^{H_i} / \alpha_m^{H_i})}, \quad i = 0, 1, \quad (\text{A.2})$$

where $\alpha_m^{H_i}$ is defined in (22). For the general case of $z = \sum_{m=1}^M \alpha_m^{H_i} x_m^2$ where $\alpha_m^{H_i}$ are distinct with $\alpha_m^{H_i} > 0$, and x_m^2 are IID with PDF of Chi-Squared with two DOF, the PDF of z is given by

$$P_z(z) = \int_{-\infty}^{\infty} \prod_{m=1}^M \frac{1}{1 - j\alpha_m^{H_i} \omega} e^{-j\omega z} \frac{d\omega}{2\pi} dz$$

$$= \begin{cases} \sum_{m=1}^M \frac{A_m^{H_i}}{\alpha_m^{H_i}} e^{-z/\alpha_m^{H_i}}, & z > 0, \\ 0, & z < 0. \end{cases} \quad (\text{A.3})$$

Thus, the performance of EC can be represented in closed form as

$$P_{fa} = \sum_{m=1}^M A_m^{H_0} \exp\left(\frac{-\gamma}{\alpha_m^{H_0}}\right),$$

$$P_d = \sum_{m=1}^M A_m^{H_1} \exp\left(\frac{-\gamma}{\alpha_m^{H_1}}\right). \quad (\text{A.4})$$

List of variables:

$\mathbf{p}(t)$:	Position vector of a moving antenna
$r(t)$:	Complex baseband signal received by an antenna
$s_o(t)$:	Deterministic component of the received signal
$A(\mathbf{p}(t))$:	Channel response to the signal at the antenna position of $\mathbf{p}(t)$
$w(t)$:	Additive noise
H_0 :	State that the received signal and replica are not synchronized
H_1 :	State that the received signal and replica are synchronized
x_m :	Correlator output of the m th subinterval
σ_A^2 :	Variance of the channel gain
σ_w^2 :	Variance of noise
\mathbf{C}_A :	Spatial covariance matrix of the channel gains
\mathbf{C}_s :	Signal covariance matrix
\mathbf{C}_w :	Noise covariance matrix
ρ_s :	Required average SNR for the static antenna
ρ_{EC} :	Required average SNR for the synthetic array with the EC process
ρ_{EG} :	Required average SNR for the synthetic array with the EG process
Ψ :	Correlation coefficient matrix
z_s :	Test statistics of the static antenna
z_{EC} :	Test statistics of the synthetic array for the EC process
z_{EG} :	Test statistics of the synthetic array for the EG process
T :	Snapshot interval in seconds
ΔT :	Snapshot subinterval in seconds
M :	Number of subintervals
J_0 :	zero-order Bessel function of the first kind
κ :	Carrier wavelength
G_{EC} :	Processing gain of the SA over the static antenna with the EC process
G_{EG} :	Processing gain of the SA over the static antenna with the EG process
ϕ :	Characteristic function
λ_s :	Eigenvalues of signal covariance matrix.

References

- [1] J. D. Parsons, *The Mobile Radio Propagation Channel*, John Wiley & Sons, New York, NY, USA, 2nd edition, 2000.
- [2] T. S. Rappaport, *Wireless Communications: Principles and Practice*, Prentice-Hall, Englewood Cliffs, NJ, USA, 2nd edition, 2002.
- [3] C.V. Rensburg and B. Friedlander, "Transmit diversity for arrays in correlated Rayleigh fading," *IEEE Transactions on Vehicular Technology*, vol. 53, no. 6, pp. 1726–1734, 2004.
- [4] B. Friedlander and S. Scherzer, "Beamforming versus transmit diversity in the downlink of a cellular communications system," *IEEE Transactions on Vehicular Technology*, vol. 53, no. 4, pp. 1023–1034, 2004.

- [5] K. N. Le, "BER of OFDM in rayleigh fading environments with selective diversity," *Wireless Communications and Mobile Computing*. In press.
- [6] J. Hu and N. C. Beaulieu, "Accurate closed-form approximations for the performance of equal gain combining diversity systems in Nakagami fading channels," *European Transactions on Telecommunications*, vol. 19, no. 6, pp. 707–717, 2008.
- [7] J. S. Colburn, Y. Rahmat-Samii, M. A. Jensen, and G. J. Pottie, "Evaluation of personal communications dual-antenna handset diversity performance," *IEEE Transactions on Vehicular Technology*, vol. 47, no. 3, pp. 737–746, 1998.
- [8] S. Kim, "Acquisition performance of CDMA systems with multiple antennas," *IEEE Transactions on Vehicular Technology*, vol. 53, no. 5, pp. 1341–1353, 2004.
- [9] R. M. Narayanan, K. Atanassov, V. Vladimir, and G. R. Kadambi, "Polarization diversity measurements and analysis for antenna configurations at 1800 MHz," *IEEE Transactions on Antennas and Propagation*, vol. 52, no. 7, pp. 1795–1810, 2004.
- [10] J. F. Valenzuela-Valdes, M. A. Garcia-Fernandez, A. M. Martinez-Gonzalez, and D. Sanchez-Hernandez, "The role of polarization diversity for MIMO systems under rayleigh-fading environments," *IEEE Antennas and Wireless Propagation Letters*, vol. 5, pp. 534–536, 2006.
- [11] S. Stergiopoulos and H. Urban, "A new passive synthetic aperture technique for towed arrays," *IEEE Journal of Oceanic Engineering*, vol. 17, no. 1, pp. 16–25, 1992.
- [12] Y. L. Jong and M. Herben, "High-resolution angle of arrival measurement of the mobile radio channel," *IEEE Transactions on Antennas and Propagation*, vol. 47, no. 11, pp. 1677–1687, 1999.
- [13] A. Broumandan, T. Lin, A. Moghaddam, D. Lu, J. Nielsen, and G. Lachapelle, "Direction of arrival estimation of GNSS signals based on synthetic antenna array," in *Proceedings of the 20th International Technical Meeting of the Satellite Division of the Institute of Navigation (ION GNSS '07)*, Fort Worth, Tex, USA, September 2007.
- [14] A. Broumandan, J. Nielsen, and G. Lachapelle, "Signal detection performance in rayleigh multipath fading environments with a moving antenna," *IET Signal Processing Journal*. In press.
- [15] S. Hyeon, Y. Yun, H. Kim, and S. Choi, "Phase diversity for an antenna-array system with a short interelement separation," *IEEE Transactions on Vehicular Technology*, vol. 57, no. 1, pp. 206–214, 2008.
- [16] Y. Wang and J. R. Cruz, "Performance enhancement of CDMA cellular systems with augmented antenna arrays," *IEEE Journal on Selected Areas in Communications*, vol. 19, no. 6, pp. 1052–1060, 2001.
- [17] S. M. Kay, *Fundamentals of Statistical Signal Processing Detection Theory*, Prentice-Hall, Englewood Cliffs, NJ, USA, 1998.
- [18] A. Broumandan, J. Nielsen, and G. Lachapelle, "Narrowband signal detection in correlated rayleigh fading with a moving antenna," in *Proceedings of the 13th International Symposium on Antenna Technology and Applied Electromagnetics (ANTEM '09) and the Canadian Radio Sciences Meeting (URSI/CNC '09)*, Banff, Canada, February 2009.
- [19] H. L. V. Trees, *Detection, Estimation, and Modulation Theory, Part I*, John Wiley & Sons, New York, NY, USA, 2001.
- [20] H. L. V. Trees, *Optimum Array Processing, Part IV, Detection, Estimation, and Modulation Theory*, John Wiley & Sons, New York, NY, USA, 2002.
- [21] J. Liberti and T. S. Rappaport, *Smart Antennas for Wireless Communications: IS-95 and Third Generation CDMA Applications*, Prentice-Hall, Englewood Cliffs, NJ, USA, 1999.